Skeletal Radiol (1989) 18:253–259

Skeletal Radiology

Fibrous metaphyseal defects

Magnetic resonance imaging appearances

P. Ritschl, M.D.[1], P.C. Hajek, M.D.[2], and Ursula Pechmann, M.D.[3]

[1] Orthopaedic Department, University of Vienna
[2] Central Institute for Radiodiagnostic, University of Vienna
[3] Institute of Anatomy, University of Vienna, Austria

Abstract. Sixteen patients with fibrous metaphyseal defects were examined with both plain radiography and magnetic resonance (MR) imaging. Depending on the age of the fibrous metaphyseal defects, characteristic radiomorphologic changes were found which correlated well with MR images. Following intravenous Gadolinium-DTPA injection, fibrous metaphyseal defects invariably exhibited a hyperintense border and signal enhancement. Healed lesions exhibited a transition to normal bone marrow. A line through the maximum longitudinal diameter of a fibrous metaphyseal defect invariably led to a point of tendinous or ligamentous insertion. Coronal MR images demonstrated the maximum longitudinal extension and the respective inserting tendon or ligamentous structure at the epiphyseal line.

Key words: Fibrous metaphyseal defect – Magnetic resonance imaging – Determination of origin

Fibrous metaphyseal defects are found at adolescence and occur at characteristic points on the circumference of long bones [1, 14, 15]. Depending on age, their distance from the epiphyseal line varies [11, 12, 14]. The longitudinal axis of fibrous metaphyseal defects in the direction of the epiphysis encounters a tendon or ligamentous structure inserting at the epiphyseal line. This structure inserts at the perichondrium of the epiphyseal cartilage and the surrounding periosteum seems to be associated with the pathogenesis of fibrous metaphyseal defects [13]. Recent investigations have shown a characteristic radiomorphologic course of fibrous metaphyseal defects in stages [12]. At stage A, they are located near the epiphyseal plate [14, 15], have a round to oval shape with a fine sclerotic margin. Stage B represents a polycyclic form, delineated by a distinct sclerotic margin. The cortex often bulges like an hourglass. Stage C, which indicates the beginning of the healing process, shows increasing mineralization which characteristically starts diaphyseally and progresses towards the epiphyseal plate [5, 12]. By stage D the fibrous metaphyseal defect has become completely sclerotic. By means of coronal and axial magnetic resonance (MR) images we demonstrate the various stages and evaluate their related tendon insertions in the region of the epiphyseal plate.

Address reprint requests to: P. Ritschl, M.D., Orthopaedic Department, University of Vienna, A-1090 Wien

Patients and methods

Sixteen patients (12 males and 4 females) with fibrous metaphyseal defects at various locations were included in this study. The average age was 17.1 years (range 11 to 23 years). Table 1 records sex, age, location, the associated tendon, stage, and total time of clinical and radiological observation. Each lesion was radiographed conventionally in two planes. MR examinations were performed on a 1.5 T superconducting magnet (Magneton, Siemens, Erlangen, FRG) in 3 mm slices according to the long axis of each fibrous metaphyseal defect using various types of surface coils. The following spin-echo sequences were employed (TR/TE):

700 ms/25 ms = T1-weighted (T1w)
2000 ms/22 ms/70 ms = balanced and T2-weighted (T2w)

Imaging matrix was 256 × 256.

In three patients (fibrous metaphyseal defects stage B), T1-weighted examinations were performed before and after i.v. injection of Gadolinium-DTPA (Magnevist, Schering, Berlin FRG).

Results

Based on the criteria found in plain radiographs [12] we identified one fibrous metaphyseal defect

Table 1. See text

Patient	Sex	Age at MR examination (years)	Location	Stage of fibrous metaphyseal defect at MR examination	Total observation period in months	Tendon insertion
A.D.	M	23	distal tibia lateral	D	40	posterior tibiofibular syndesmosis
E.A.	M	21	distal femur medial	B	7	adductor magnus muscle
F.R.[a]	M	20	distal femur medial (2×) +lateral (2×)	D	35	gastrocnemius muscle, medial head (2×) gastrocnemius muscle, lateral head (2×)
G.M.	M	16	distal femur medial	B	5	adductor magnus muscle
H.B.	F	16	distal femur medial	C	5	gastrocnemius muscle, medial head
J.M.	M	15	right fibula	fracture	18	anterior ligament of head of fibula
L.F.	M	22	distal tibia lateral	B	24	anterior tibiofibular syndesmosis
M.R.[a]	M	11	distal femur medial and lateral	A	11	gastrocnemius muscle, medial head, iliotibial tract, proximal insertion
M.A.	F	17	distal femur medial	C	7	gastrocnemius muscle, medial head
M.E.	M	19	distal femur medial	B	26	adductor magnus muscle
P.T.	M	12	distal femur lateral	B	8	iliotibial tract, proximal insertion
P.R.	M	15	proximal tibia lateral	B	3	iliotibial tract Gerdy tubercle
R.G.[a]	M	16	distal femur lateral, medial	C	35	adductor magnus muscle gastrocnemius muscle, lateral head
S.H.	M	21	distal femur lateral	B	27	gastrocnemius muscle, lateral head
St.E.[a]	F	14	proximal fibula medial and lateral	C	19	anterior ligament of head of fibula, biceps muscle of thigh
St.G.	F	15	proximal tibia medial	C	2	semimembranosus muscle

[a] Patients with multiple metaphyseal defects

at stage A, seven at stage B, five at stage C, and another two at stage D. Staging of one lesion of the fibula was not possible due to secondary fracture. All 16 fibrous metaphyseal defects could be visualized on MR images. Their locations and the associated tendon insertions, which all could be demonstrated on MR images, are shown in Table 1. Four patients exhibited multiple metaphyseal defects (Table 1). According to stage, the fibrous metaphyseal defects exhibited a variable appearance.

Stage A (Fig. 1A) (one patient): A longitudinal lesion with smooth borders; relatively homogeneous but with variable signal intensity – from very high – similar to that of fat, to intermediate – comparable to muscle. Occasionally, thin linear structures of very low signal intensity were encountered (Fig. 1B).

Stage B (Fig. 2A) (seven patients): These showed an increasingly inhomogeneous structure; the total number of linear structures of low signal intensity increased remarkably, leading to an increasing division into many small roundish areas of varying signal intensity on T1-weighted images (Fig. 2B). The diaphyseal part of the lesion at this stage showed multiple small (1–5 mm) areas which exhibited intermediate to low signal intensity on T1w and T2w images. Following i.v. injection of Gd-DTPA, fibrous metaphyseal defects invariably exhibited thin hyperintense borders. Furthermore, a few small areas of low signal intensity showed distinct signal enhancement (Fig. 5).

Stage C (Fig. 4A) (five patients): All the characteristics of stage B were present in a more pronounced way (Fig. 4B). The margins were formed by a more than 1 mm thick border of very low signal intensity (T1w and T2w images) (Fig. 5). This correlated with the bulging sclerotic margin on plain radiographs. Fibrous metaphyseal defects at this stage were clearly recognizable in their full extent on MR images. Overall their signal intensity was very low on T1w images. On plain radiographs, these areas corresponded with zones where the borders

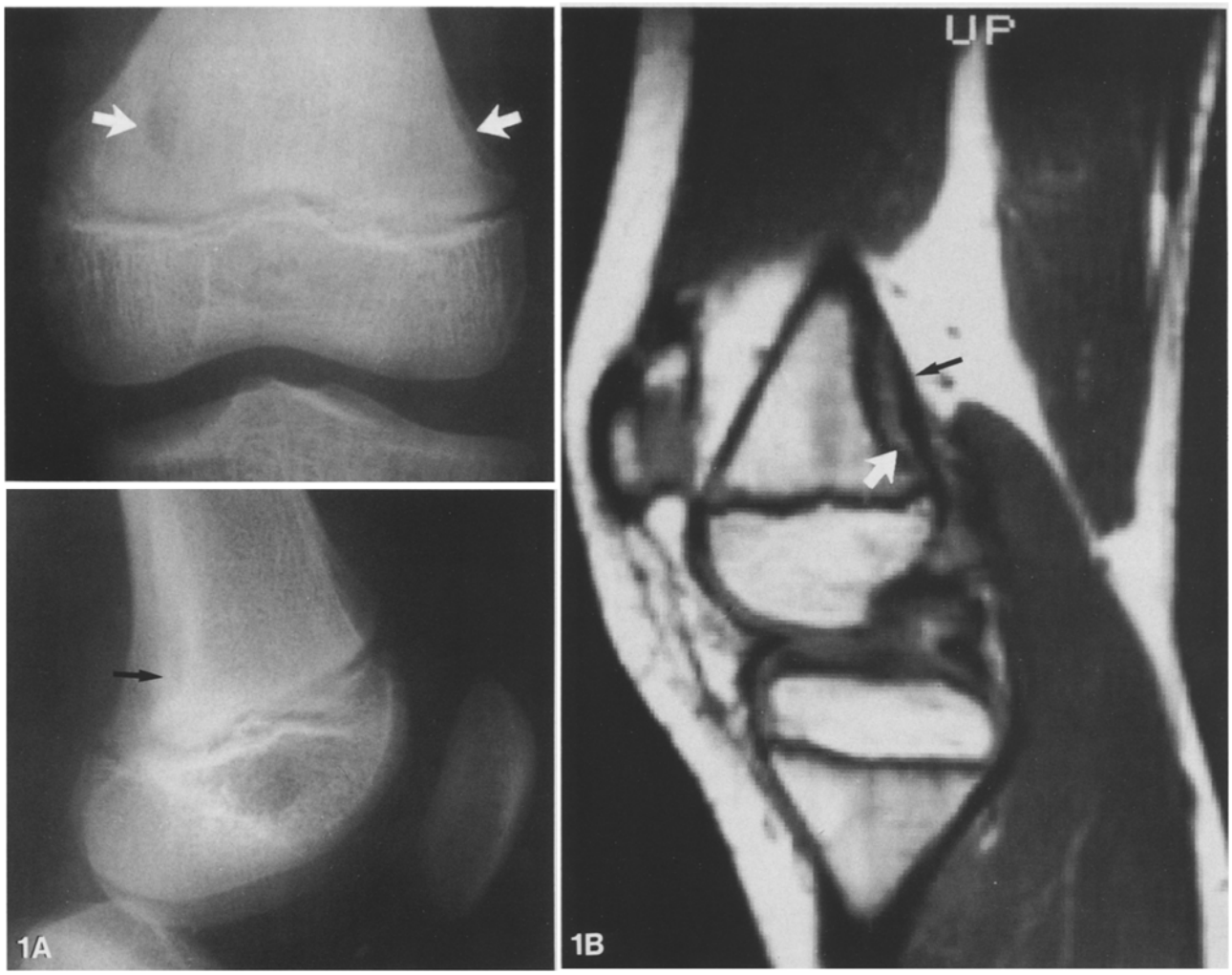

Fig. 1 A, B. *MR 11-year-old-male.* **A** Radiograph (anteroposterior, lateral) of the distal femur, two fibrous metaphyseal defects (medio- and latero-dorsal) at stage A. Each lesion (→), located in close proximity to the epiphyseal plate, has an oval shape and is surrounded by a thin sclerotic margin. **B** Parasagittal MRI (SE 700/15) through distal femur. The fibrous metaphyseal defect (→) at stage A shows a relatively homogeneous structure of medium to high (⇒) signal intensity with a margin of low signal intensity

Fig. 2 A, B. *LF 22-year-old-male.* **A** Plain radiograph (anteroposterior) of the distal tibia. The fibrous metaphyseal defect (stage B) is polycyclic, sharply delimited, and shows pseudotrabeculae. The maximum longitudinal diameter of the lesion points toward the insertion of the anterior tibiofibular ligament. **B** Coronal MRI (SE 700/15) through distal tibia. The fibrous metaphyseal defect (stage B) shows small areas of varying signal intensities subdivided by thin low-signal pseudotrabeculae (→). A thin, sharply delineated border is seen

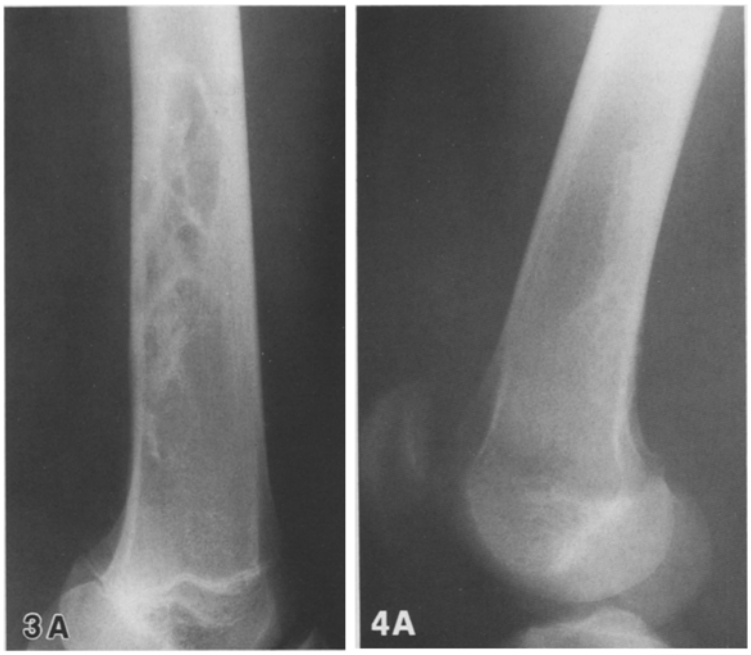

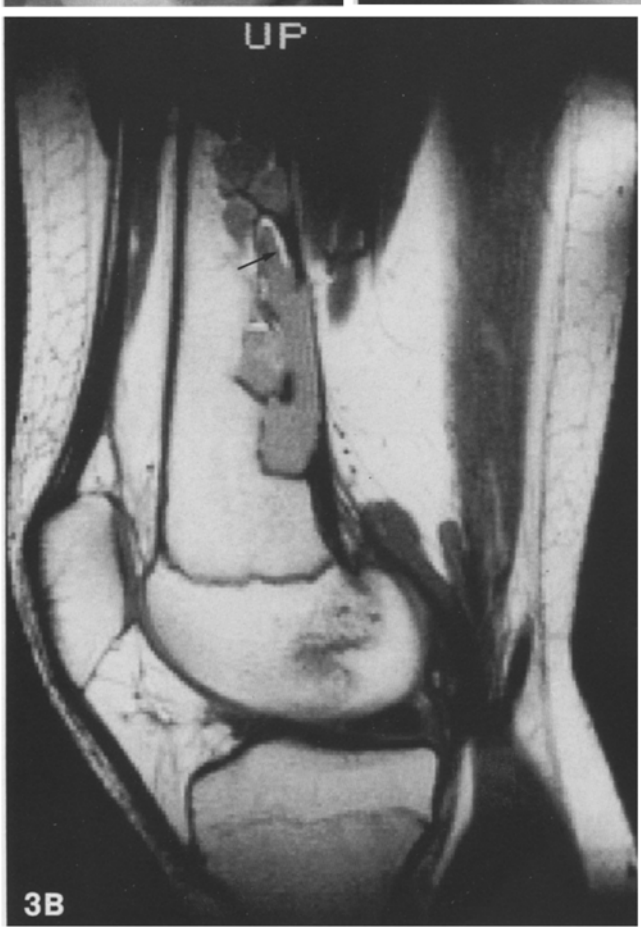

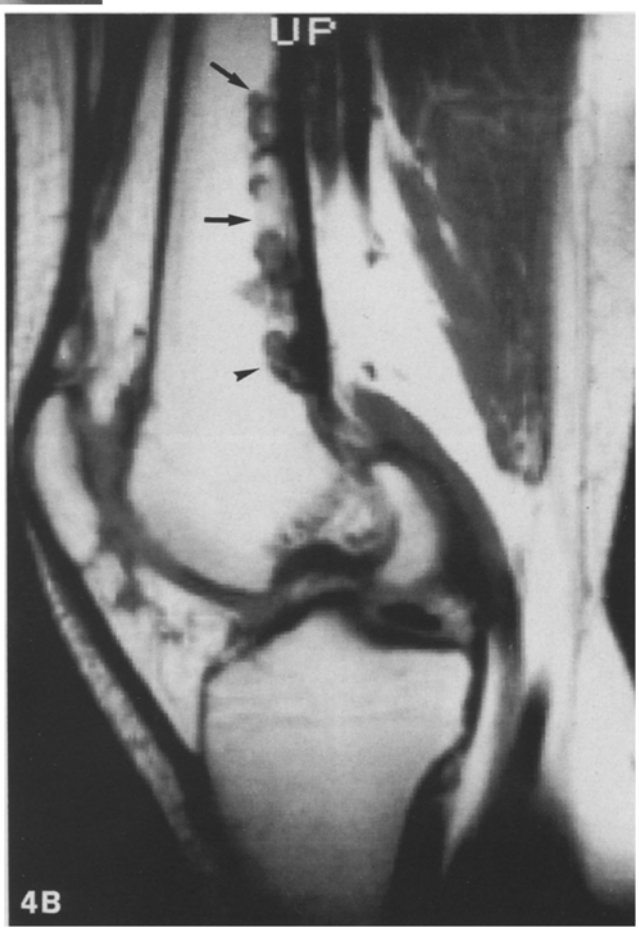

Fig. 3A, B. *HB 16-year-old-female.* **A** Plain radiograph (lateral) of left distal femur: fibrous metaphyseal defect at stage B. **B** Parasagittal MRI (SE 700/15) through the distal femur. The fibrous metaphyseal defect (stage B) displays multiple areas of homogeneous structure with pseudotrabeculae. A purely cystic fibrous metaphyseal defect was verified operatively. Note chemical shift artifact (→)

Fig. 4A, B. *MA, 17-year-old-female.* **A** Plain radiograph (lateral) of fibrous metaphyseal defect at stage C. Mineralization increases from epiphyseal to diaphyseal poles. **B** Sagittal MRI (SE 700/15) through the distal femur. The fibrous metaphyseal defect (stage C) exhibits an inhomogeneous structure with numerous small areas (→) of signal equal to normal bone marrow. Close to the epiphysis, a small area with the MR characteristics of stage B is seen (→)

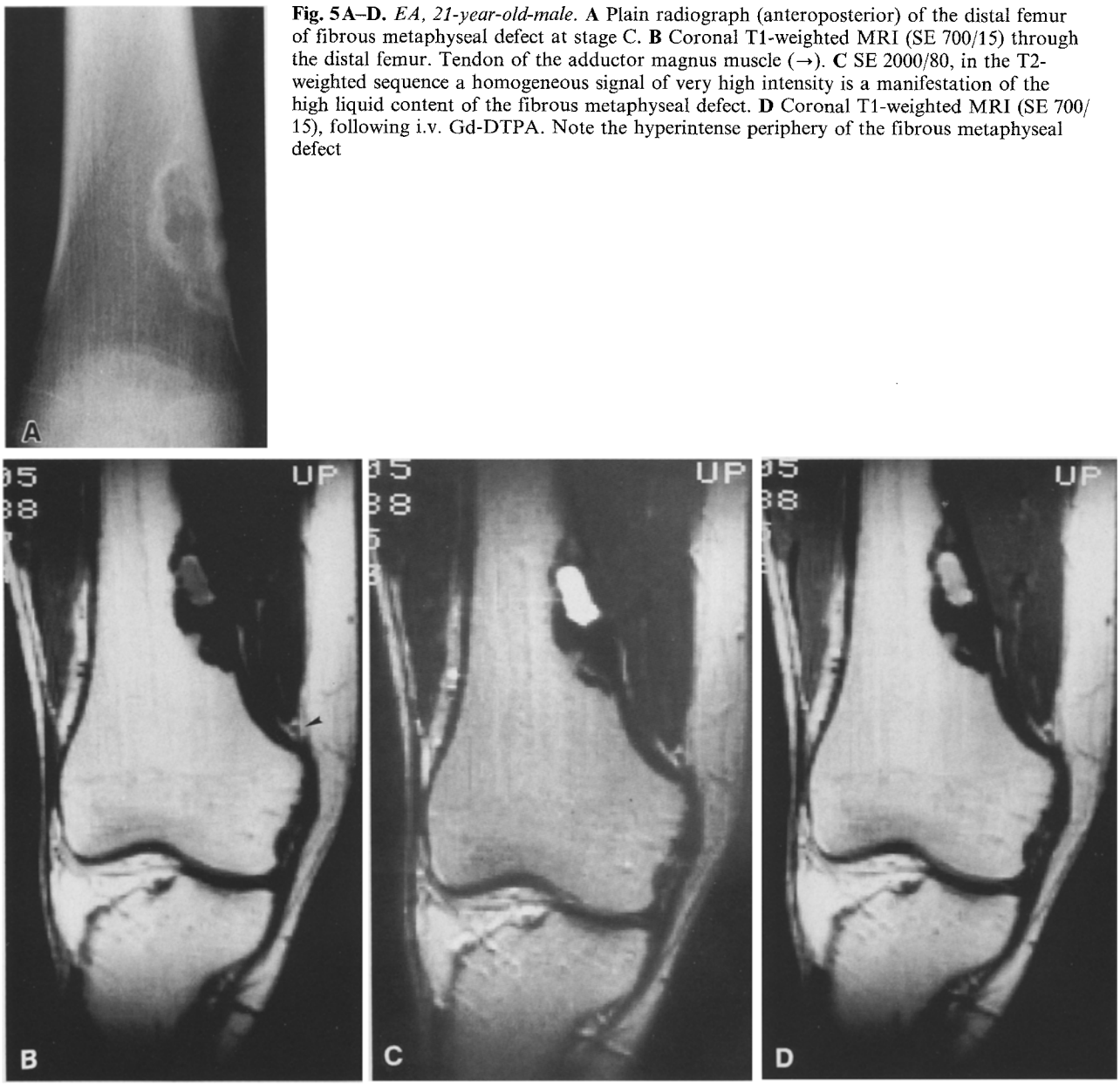

Fig. 5A–D. *EA, 21-year-old-male.* **A** Plain radiograph (anteroposterior) of the distal femur of fibrous metaphyseal defect at stage C. **B** Coronal T1-weighted MRI (SE 700/15) through the distal femur. Tendon of the adductor magnus muscle (→). **C** SE 2000/80, in the T2-weighted sequence a homogeneous signal of very high intensity is a manifestation of the high liquid content of the fibrous metaphyseal defect. **D** Coronal T1-weighted MRI (SE 700/15), following i.v. Gd-DTPA. Note the hyperintense periphery of the fibrous metaphyseal defect

close to the diaphysis meet normal bone. In this zone, MR images occasionally exhibit small areas with the typical signal behavior of normal bone marrow. The areas near the epiphysis resembled stage B.

Stage D (two patients): Two different appearances were found: one appeared as a homogeneous, very low signal intensity, which corresponded to the sclerotic zone at plain radiographs. The second was characterized by an indistinct delineation against surrounding bone (Fig. 6A), which correlated with the progressive disappearance of the lesion on the plain radiograph. This form was clearly visible on MR images as of homogeneous low signal intensity. During healing, an increasingly normal appearing bone marrow structure and signal intensities equal to yellow bone marrow were found, which invariably started from the diaphyseal side (Fig. 6B).

Discussion

Fibrous metaphyseal defects are found in quite characteristic locations on the circumference of long bones. An imaginary straight line along the maximum longitudinal extension of a lesion will meet the insertion of a tendon or ligamentous

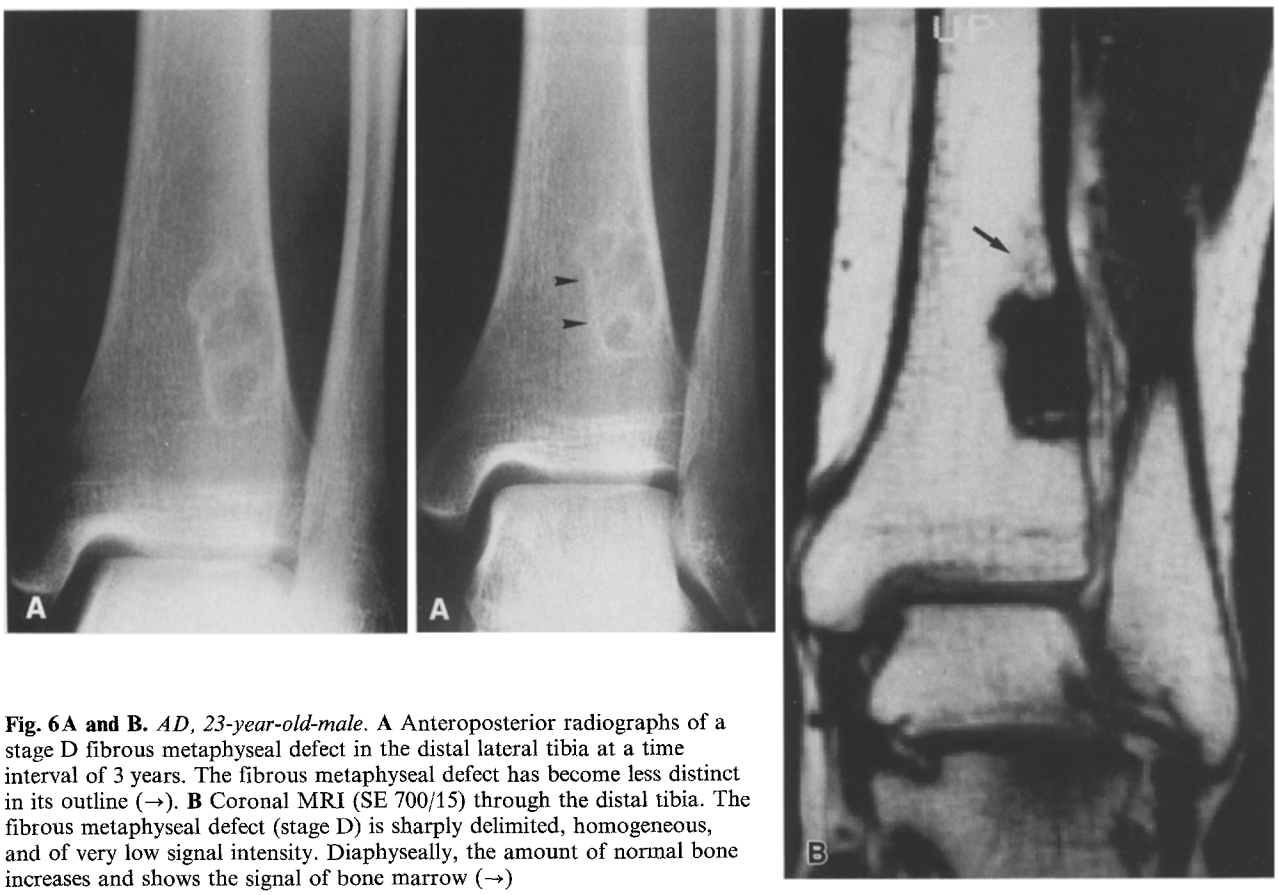

Fig. 6A and B. *AD, 23-year-old-male.* **A** Anteroposterior radiographs of a stage D fibrous metaphyseal defect in the distal lateral tibia at a time interval of 3 years. The fibrous metaphyseal defect has become less distinct in its outline (→). **B** Coronal MRI (SE 700/15) through the distal tibia. The fibrous metaphyseal defect (stage D) is sharply delimited, homogeneous, and of very low signal intensity. Diaphyseally, the amount of normal bone increases and shows the signal of bone marrow (→)

Table 2. Tendons or ligaments inserting at the perichondrium of the epiphyseal plate

Knee joint:
a) *distal femur medial*
adductor magnus muscle
gastrocnemius muscle, medial head
b) *distal femur lateral*
proximal insertion, iliotibial tract (Kaplan-Fasern) [6]
gastrocnemius muscle, lateral head
c) *proximal tibia medial*
semimembranosus muscle
d) *proximal tibia lateral*
iliotibial tract
anterior and posterior ligament of head of fibula
e) *proximal fibula medial*
anterior and posterior ligament of head of fibula
f) *proximal fibula, lateral*
biceps femoris muscle
Ankle joint:
a) *distal tibia lateral*
tibiofibular syndesmosis
(anterior and posterior tibiofibular ligament)

structure at the epiphyseal plate (Table 2) [11, 12]. Initially fibrous metaphyseal defects are found very close to the epiphyseal plate [12, 15] in direct relation to such an insertion. Therefore it seems reasonable to conclude, that such an insertion – via an additional pathogenetic factor – may be related to the development of a fibrous metaphyseal defect. Using MR images through the longitudinal axis of the fibrous metaphyseal defect, it was possible to visualize consistently the causal tendon and its insertion into the epiphyseal plate (Table 1).

The MR appearance of fibrous metaphyseal defects at Stages A and B was characterized by high signal intensities of varying homogeneity. This high signal is comparable to the histology of these lesions, which for the most part consist of fibrous structures with a varying content of fat-storing foam cells. These areas showed a reduced signal intensity on T2w images, corresponding to the signal behavior of intracellular fatty substances stored in foam cells and the intracellular hemosiderin of stromal cells [2–5, 7, 9, 16]. Low-signal linear structures correspond to the formation of fibrous septa or osseous pseudosepta [8].

Diaphyseal mineralization, caused by progressive healing, exhibited predominantly low signal intensity on MR images at stages C and D. As demonstrated, healing appeared focal, starting from the diaphyseal part of the lesion. A second

form of healing seen on MR scans and plain radiographs (Fig. 6A) (→) was diffuse loss of clarity.

Following i.v. injection of Gd-DTPA, the central portion of a fibrous metaphyseal defect produced generally no increase in signal intensity on T1w images. Occasionally, a slight increase was found in areas of medium signal intensity. This phenomenon might be caused by small hypervascularized area [10]. The margins invariably showed a ring-like signal increase, consistent with thin hypervascularized zones at the periphery (Fig. 5D).

Using MR images through the longitudinal axis of the fibrous metaphyseal defect, it was possible consistently to visualize a tendon and its insertion into the epiphyseal plate (Table 1). This suggests a close association of fibrous metaphyseal defects and an inserting tendon at the epiphyseal plate and supports our theory about the possible origin of fibrous metaphyseal defects [13].

In conclusion, fibrous metaphyseal defects exhibit MR appearances differing with their stage. On the rare occasion when standard radiography is not diagnostic, MRI might prove a satisfactory supplementary method of imaging.

References

1. Caffey J (1955) On fibrous defects in cortical walls of growing tubular bone: their radiologic appearance, structure prevalence, natural course and diagnostic significance. Adv Pediatr 7:13
2. Dahlin DC, Unni KK (1986) Metaphyseal fibrous defect. Bone tumors. Thomas, Springfield, p 149
3. Dominok GW, Knoch HG (1977) Knochengeschwülste und geschwulstähnliche Knochenerkrankungen. Fischer, Jena, p 174
4. Huvos AG (1979) Bone tumors: diagnosis, treatment and prognosis. Saunders, Philadelphia, p 297
5. Jaffe HL (1959) Tumors and tumorous conditions of the bone and joints. Lea & Febiger, Philadelphia, p 76
6. Kaplan EB (1958) The iliotibial tract. Clinical and morphological significance. J Bone Joint Surg [Am] 10:817
7. Kotz R, Kogelnik HD, Immenkamp M, Lechner G, Müller K, Salzer M, Salzer-Kuntschik M, Weber U (1984) Tumore und tumorähnliche Erkrankungen. In: Hackenbroch M, Hupfauer W, Witt AN, Rettig H, Schlegel KF (eds) Orthopädie in Praxis und Klinik, Bd. III, Teil II: Allgemeine Orthopädie. Thieme, Stuttgart, p 301
8. Lichtenstein L (1972) Bone tumors, 4th edn: Nonosteogenic fibroma of bone tumors. Mosby, St. Louis, p 121
9. Mirra JM, Gold, RH, Rand F (1982) Disseminated nonossifying fibromas in association with café-au-lait spots (Jaffe-Campanacci syndrome). Clin Orthop 168:192
10. Mucchi L, Goidanich IF, Zanoli S (1966) Angiographie in der Knochenpathologie. Thieme, Stuttgart
11. Ritschl P, Karnel F (1986) Zur Pathogenese des fibrösen Kortikalisdefektes und nicht ossifizierenden Knochenfibromes. Z Orthop 124:671
12. Ritschl P, Karnel F, Hajek P (1988) Fibrous metaphyseal defects – determination of their origin and natural history using a radiomorphological study. Skeletal Radiol 17:8
13. Ritschl P, Lintner F, Pechmann U, Brand G (in press) Fibrous metaphyseal defect – A new concept of origin. Int Orthop
14. Selby S (1961) Metaphyseal cortical defect in the tubular bones of growing children. J Bone Joint Surg [Am] 43: 395
15. Sontag LW, Pyle SI (1941) The appearance and nature of cyst-like areas in the distal femoral metaphyses of children. AJR 46:185
16. Spjut HJ, Dorfman HD, Fechner RE, Ackerman L v. (1970) Tumors of bone and cartilage. Atlas of tumor pathology, Armed Forces Institute of Pathology, Washington, D.C. p 254